ISSN 1027-5495. Functional Materials, 33, No.1 (2026), p. 98-105
doi:http://dx.doi.org/10.15407/fm33.01.98

Temperature dependent thermo-mechanical properties of 3C and 6H silicon carbide from atomistic simulations on large-scale systems with DFT-derived machine learning interatomic potential

Oleksandr Parfionov*, Oleksandr Vasiliev

Frantsevich Institute for Problems of Materials Science NASU,
O. Pritsaka street 3, Kyiv, 03142, Ukraine
* o.parfionov@ipms.kyiv.ua
Received September 16, 2025, approved January 20, 2026

This work presents a comprehensive, comparative study of two primary SiC polytypes, cubic (3C) and hexagonal (6H), using large-scale molecular dynamics simulations powered by a high-fidelity Machine Learning Interatomic Potential (MLIP) trained on a custom dataset of 5152 first-principles configurations. We present a complete set of thermo-mechanical properties, including the coefficient of thermal expansion (CTE) and the full elastic tensor (C_{ij}), from 0 K to 2000 K. A crucial finding from the analysis of the uniaxial Young's modulus is that the 6H polytype undergoes thermal softening at a rate of approximately 49 MPa/K, which is almost twice as fast as the 3C polytype at 25 MPa/K. This pronounced single-crystal anisotropy contrasts with the behavior of the Voigt-Reuss-Hill averaged polycrystalline moduli, which show similar softening rates of ~33 MPa/K for both materials. The presented properties are validated against established experimental and theoretical data, providing a quantitative understanding of thermo-mechanical behavior behavior of SiC and delivering the essential property data needed to enhance the fidelity of engineering models for SiC components.
Keywords: Elastic Constants, Thermo-mechanical Properties, DFT, Silicone Carbide, Machine Learning Interatomic Potentials

Температурно-залежні термомеханічні властивості карбіду кремнію 3C та 6H, отримані за допомогою атомістичного моделювання систем великого масштабу з використанням міжатомного потенціалу машинного навчання, навченого на даних DFT розрахунків. *О. Парфьонов, О. Васильєв*

Представлено комплексне порівняльне дослідження двох основних політипів SiC — кубічного (3C) та гексагонального (6H) — із застосуванням моделювання на великому масштабі з використанням міжатомного потенціалу машинного навчання високої точності. Потенціал було навчено на спеціально створеному наборі даних із 5152 конфігурацій, розрахованих із перших принципів. Визначено повний набір термомеханічних властивостей, зокрема коефіцієнт теплового розширення (КТР) та повний тензор пружності (C_{ij}), в діапазоні температур від 0 до 2000 К. Ключовим результатом є аналіз одновісного модуля Юнга: встановлено, що політип 6H зазнає термічного розм'якшення зі швидкістю приблизно 49 МПа/К, що майже вдвічі перевищує показник політипу 3C (25 МПа/К). Така виражена анізотропія монокристалів контрастує з поведінкою полікристалічних модулів (усереднених за методом Фойгта–Ройса–Гілла), які демонструють близькі значення швидкості розм'якшення (~33 МПа/К) для обох політипів. Отримані результати валідовано шляхом порівняння з наявними експериментальними і теоретичними даними. Дана робота забезпечує кількісне розуміння термомеханічної поведінки SiC та надає необхідні дані для підвищення точності інженерних моделей компонентів із карбіду кремнію.

1. Introduction

Silicon Carbide (SiC) has become one of the leading wide-bandgap semiconductor and advanced ceramic, known for its exceptional combination of properties including high strength, hardness, thermal conductivity, and resistance to chemical and radiation degradation. These attributes make it an enabling material for applications in extreme environments where conventional materials fail, such as components for nuclear reactors [1], thermal protection systems for hypersonic vehicles [2], and high-efficiency power electronics [3].

One of the defining characteristic of SiC is polytypism, the ability to crystallize into numerous distinct structures with different stacking sequences of Si-C bilayers. Although there are more than 250 polytypes [4], the cubic zinc-blende (3C-SiC) and hexagonal (4H- and 6H-SiC) structures are of the greatest technological significance. These subtle structural differences result in different electronic and mechanical properties, so direct comparison of their behavior is important for material selection and device design.

For high temperature applications, the change in mechanical properties with temperature is critical to design. The universal phenomenon of thermal softening – a decrease in elastic moduli with increasing temperature – ultimately limits the operational range of any component. Although this behavior is qualitatively understood for SiC, a systematic and comparative datasets quantitatively describing the thermoelastic response of different polymorphs remain extremely rare in the literature. These data are necessary to determine the governing laws of thermoelasticity, used in finite element models for predicting the service life and reliability of components [5]. Furthermore, these fundamental elastic constants are crucial for a variety of other physical models, including the prediction of anisotropic sound velocities, dislocation dynamics, and ideal material strength [6, 7].

Molecular dynamics (MD) simulations on large systems (>1000 atoms) is a powerful atomistic tool to investigate the above properties. However, the accuracy of MD is entirely dependent on the fidelity of the underlying interatomic potential. Although classical potentials like Tersoff and Vashishta are widely used [8], they may have limitations in accurately describing the complex covalent and ionic bonds in SiC over a wide range of conditions. The recent advent of Machine Learning Interatomic Potentials (MLIPs) opens the way to achieving accuracy close to quantum density functional theory (DFT) at significantly lower computational cost [9]. This allows large systems to be simulated over long periods of time, which is necessary to obtain statistically reliable thermal and mechanical properties.

In this paper, we train and use the MLIP model on DFT data to conduct a systematic comparative study of the thermomechanical properties of 3C- and 6H-SiC. We calculate the complete temperature-dependent elastic tensor, engineering moduli, and the coefficient of thermal expansion for each of these polytypes.

2. Computational Methodology

2.1. Machine Learning Interatomic Potential (MLIP)

The Machine Learning Interatomic Potential (MLIP) used in this work was developed using the NequIP framework [10]. To ensure high fidelity, the MLIP was trained on a comprehensive, custom dataset generated from first-principles calculations. The final training set, comprising 5152 configurations, was formed based on Density Functional Theory (DFT) calculations performed with the Quantum Espresso package. These calculations employed the Perdew-Burke-Erzerhof (PBE) exchange-correlation functional [11] and Projector Augmented-Wave (PAW) pseudopotentials [12] with a plane-wave cutoff energy of 100 Ry ($2.18 \cdot 10^{-16}$ J). To enable potential transfer, the dataset was designed to cover a wide thermodynamic range, including structures obtained from variable-cell molecular dynamics simulations of various key SiC polytypes (3C, 2H, and 6H) at temperatures ranging from 10 K to 2700 K.·

2.2. Molecular Dynamics Simulations

All MD simulations were performed using the Atomic Simulation Environment (ASE) framework [13], with the validated MLIP serving as the force and stress calculator. To minimize finite-size effects and ensure that the simulation results are representative of the bulk material, large supercells containing between 2000 and 6000 atoms were constructed for both the 3C- and 6H-SiC polytypes. A Berendsen thermostat was employed in all relevant simulations to control the system's temperature.

The coefficient of thermal expansion (CTE) was determined from a series of simulations in

the isobaric-isothermal (NPT) ensemble. The systems were equilibrated at zero pressure across a range of target temperatures: 0 K to 1500 K with a step of 50 K. The average equilibrium cell parameters were recorded at each temperature to derive the CTE.

The temperature-dependent elastic constants, $C_{ij}(T)$, were calculated from simulations in the canonical (NPT) ensemble using the stress-strain method [14]. For each target temperature, the zero-pressure volume was first determined from a preceding NPT run. A series of small, finite strains (±0.5%, ±1.0% and ±1.5%) were then applied to the simulation box for each required deformation mode. The average stress tensor was calculated for each applied strain, and the elastic constants were extracted from the slope of the resulting linear stress-strain relationship. In Voigt notation, the stress and strain tensors are 6-component vectors (ε_i and ε_i, respectively), which are related to each other by elastic constants C_{ij} as follows: $\sigma_i = C_{ij}\varepsilon_i$.

To find all the unknown C_{ij} values, we need to solve this system of equations by applying a series of simple, known strain vectors ε_i and measuring the resulting stress vector σ_i. The six independent deformation modes, that were mentioned earlier, correspond to applying a small strain, one at a time, to each component of the strain vector ε_i.

Finally, to supplement and validate our primary method, additional mechanical properties were calculated. The uniaxial Young's modulus along the *c*-axis was independently determined from simulated tensile tests: for each temperature a series of strains (1000 for 1.5% total strain) was applied and the Young's modulus was defined from the slope of the stress-strain curve. From the full set of single-crystal elastic constants, the effective polycrystalline Young's modulus (*E*) and bulk modulus (*B*) were then derived using the Voigt-Reuss-Hill (VRH) averaging scheme [15, 16] for direct comparison with engineering data.

3. Results and Discussion

3.1. MLIP

Our initial strategy for developing MLIP was based on the use of publicly available data, namely training the potential on a broad set of calculations from the NOMAD open-access repository. Although the initial MLIP gave satisfactory results in predicting the coefficient of thermal expansion (CTE), subsequent validation simulations revealed a critical drawback: the calculated mechanical moduli differed significantly from the generally accepted experimental and calculated values given in the literature. This discrepancy highlighted the need to create a more specialized and robust training dataset to accurately reflect the specific interatomic forces governing elastic behavior in SiC.

To address uncertainties in the predicted mechanical properties, a more comprehensive, custom dataset was generated using density functional theory (DFT), as outlined in the Methodology section.

With this high-fidelity dataset we trained the final MLIP based on E(3)-equivariant graph architecture [10] with a cutoff radius (rmax) of 4.0 Å ($4{\cdot}10^{-10}$ m). The convergence of the process was monitored by measuring the total losses, mean absolute errors (MAE) of energy per atom and force components, as shown in Figure 1. When the validation losses reached a plateau, the values of MAEs for energy per atom and force components were 0.5 meV/atom (8·10-23 J/atom) and 4 meV/Å ($6.4{\cdot}10^{-12}$ N) respectively, matching the convergence values during the DFT calculations.

To validate the new trained potential, we first calculated the ground-state elastic properties at 10 K and 300 K. As detailed in Table 1, the MLIP now accurately reproduces the independent elastic constants for both 3C- and 6H-SiC, showing excellent agreement with established DFT and experimental values. This fundamental verification provides a high degree of confidence in the ability of the potential to accurately predict the thermomechanical properties of SiC at finite temperatures.

3.2. Thermal Expansion

The calculated coefficient of thermal expansion as a function of temperature for both 3C- and 6H-SiC is presented in Figure 2 (a, b). In Figure 2a we can see the size effects of the simulated system. As the temperature increases the fluctuations affect smaller systems more significantly whereas the much bigger system is more resilient to such effects.

Our calculated LTEC values of $5.29{\cdot}10^{-6}$ K^{-1} for 6H-SiC along c-axis is in good agreement with experimental measurements [25]. The calculated value of $6{\cdot}10^{-6}K^{-1}$ for 3C-SiC represents the average over broad temperature region. Taking into account the LTEC's strong temperature dependence [30, 35], high temperature discrete

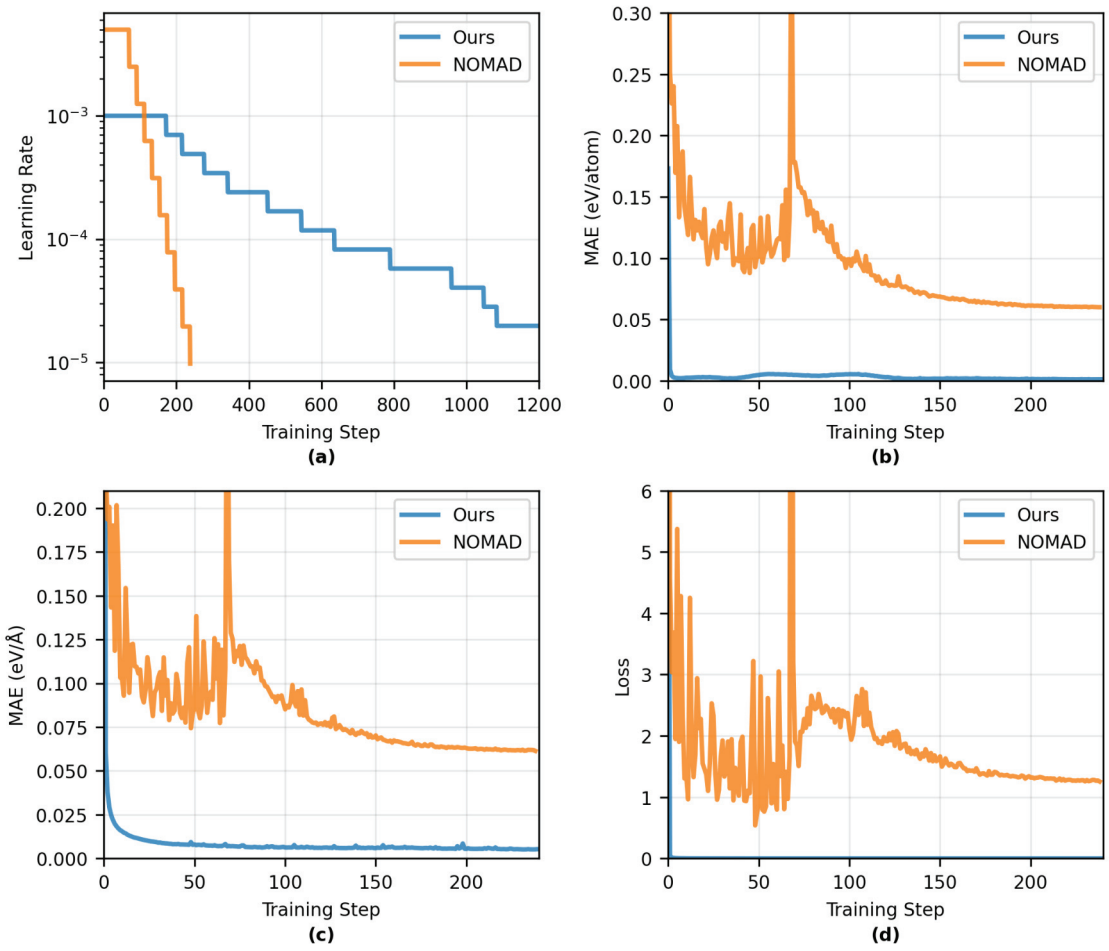

Figure 1. MLIP training metrics: learning rate (a), validation energy per atom MAE (b), validation force MAE (c) and validation loss (d).

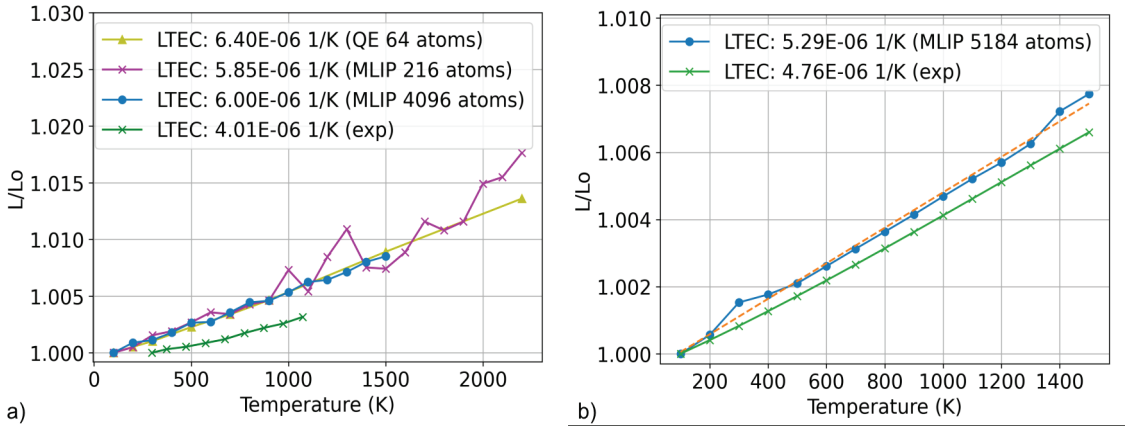

Fig. 2. Calculated rRelative cell length vs temperature along c-axis for 3C-SiC[(a) and 6H-SiC (b) with experimental data from [24] and [25] (respectively) given for comparison.

data represents the more proper comparison basis with which the calculated value is in very good agreement. The remaining discrepancy can be attributed to a known limitation of the PBE functional, which tends to overestimate lattice anharmonicity in covalent systems [34], which is further corroborated by the DFT data obtained during the dataset generation (QE in Fig. 2a).

3.3. Temperature-Dependent Elastic Properties

The full set of calculated independent elastic constants for 3C- and 6H-SiC as a function

Table 1: Validation structural and elastic properties. Comparison of MLIP predictions with DFT and experimental data.

Polytype	Property	MLIP (10 K)	DFT (0 K)	MLIP (300 K)	Exp. (300 K)
3C-SiC	C_{11}, GPa	393	385 [17] 392 [19]	382	390 [18] 395±12 [20]
	C_{12}, GPa	146	135 [17] 134 [19]	140	142 [18] 132±9 [20]
	C_{44}, GPa	249	249 [19]	243	256 [18] 236±7 [20]
6H-SiC	C_{11}, GPa	503	527 [21]	498	501±4 [22] 502±20 [23]
	C_{12}, GPa	98	107 [21]	94	111±5 [22] 95±29 [23]
	C_{13}, GPa	53	56 [21]	53	52±9 [22]
	C_{33}, GPa	574	563 [21]	552	553±4 [22] 565±11 [23]
	C_{44}, GPa	176	165 [21]	172	163±4 [22] 169±4 [23]

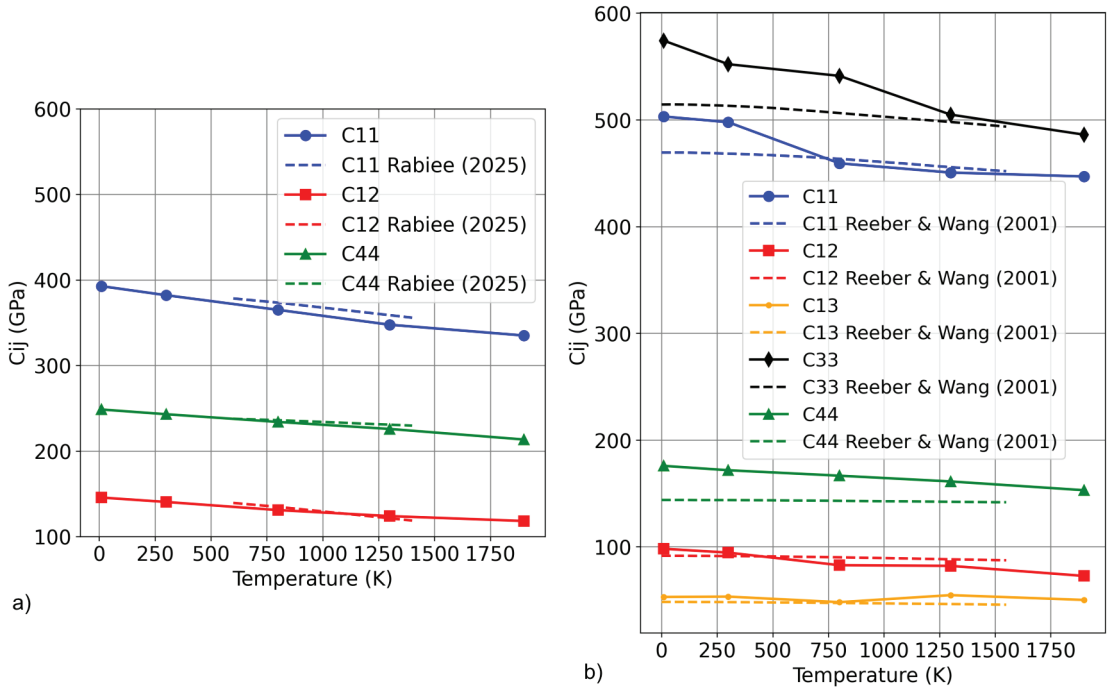

Fig. 3. Temperature dependence of elastic constants for single crystals: 3C-SiC compared to the other simulation by Rabiee (2025) [26] (a) and 6H-SiC compared to the empirical prediction method by Reeber (2001) [27] (b).

of temperature is shown in Figure 3. Our C_{ij} results for 3C-SiC (Fig. 3a) are in fairly good agreement with the simulation results from another work [26]. In Figure 3b we compare our results for 6H polytype to the results from the other work obtained by empirical prediction method [27]. Although not a perfect match, it improves at higher temperatures.

Using the Voigt-Reuss-Hill (VRH) averaging scheme [15] we can estimate the effective polycrystal values of Young's and bulk moduli. Then the calculated data can be fitted to empirical models, such as the Wachtman equation [28], to provide a simple analytical expression for use in engineering simulations:

$$E(T) = E_0 - B \cdot T \cdot exp(-T_0 / T)$$

Table 2. Wachtman equation E_0, B and T_0 fitted to the calculated Young's modulus data for 3C- and 6H-SiC.

Polytype	E_0 (GPa)	B (MPa/K)	T_0 (K)
3C-SiC	441.45	32.97	0*
6H-SiC	509.27	33.45	0*

* – the value does not account for low-temperature quantum-mechanical effects (see discussion in text).

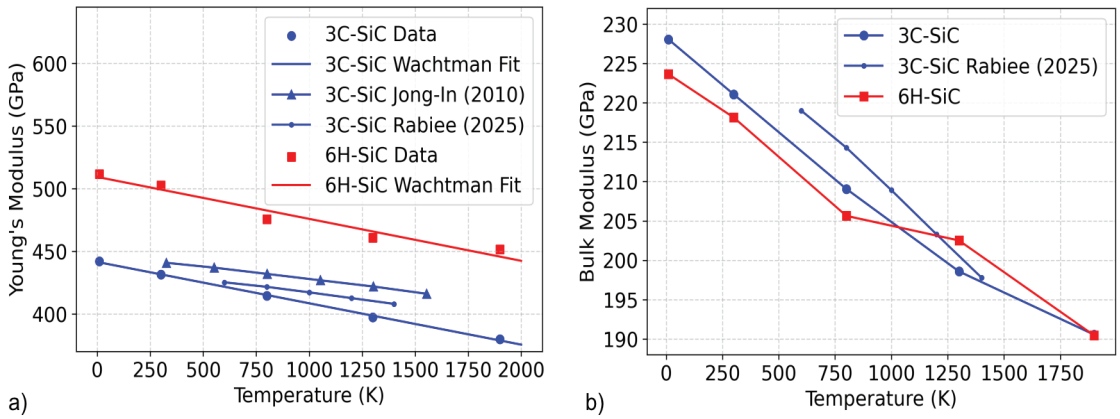

Fig. 4. Temperature dependencies of the effective polycrystalline 3C- and 6H-SiC: Young's modulus with the Wachtman fit compared to experimental by Im (2010) [29] and other simulation by Rabiee (2025) [26] data (a) and bulk modulus compared to other simulation by Rabiee (2025) [26] (b).

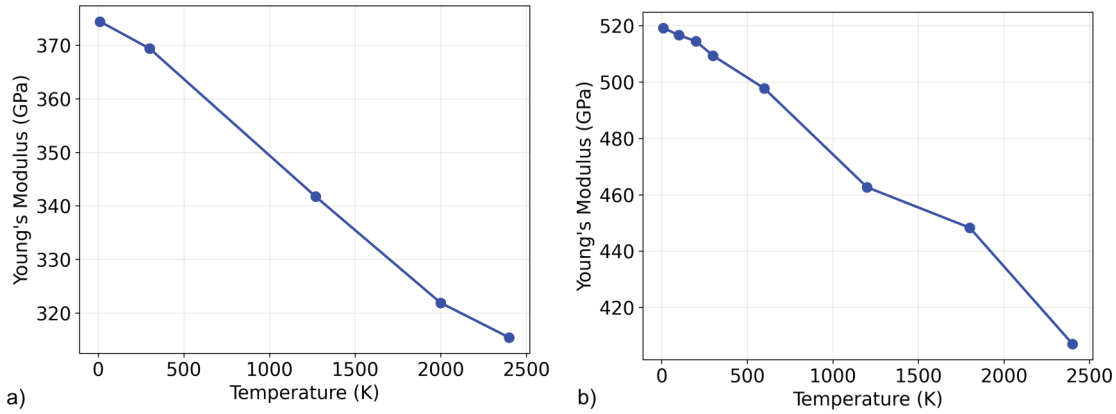

Fig. 5. Young's modulus under uniaxial loading along the c-axis for 3C-SiC (a) and 6H-SiC (b).

In Table 2 we provide values for E_0, B and T_0 as well as the fitting curves in Figure 4a.

The change of Young (Fig. 4a) and bulk (Fig. 4b) moduli is approximately linear over the majority of the temperature range investigated, which is consistent with experimental observations [30] and theoretical predictions [31] for SiC. The fitted value of $T_0 = 0$ for both polytypes is a direct consequence of the classical treatment of nuclear dynamics in MD simulations. Path-integral MD would recover the expected finite T_0 value as shown in [33], but requires significant tuning of the MLIP in the low-temperature region with marginal fidelity gains in general. Also from the values of coefficient B we can see that the softening rate for both polytypes is approximately the same(~33 MPa/K), which is notably higher than the experimentally measured rate of ~20 MPa/K for polycrystalline SiC [29] and the ~22 MPa/K obtained by Rabiee [26] using classical MD with Tersoff potential. The most probable source of the higher softening rate in our work originates from the underlying DFT description (see PBE functional discussion in 3.2). It should be noted, however, that while empirically parameterized potentials such as Tersoff may reproduce certain experimental properties more closely, the first-principles-based approach adopted here offers broader transferability and the ability to capture trends across polytypes and thermodynamic conditions on equal footing — a capability that will be further exploited in Section 3.4.,

3.4. Single-crystal Young's Modulus

The uniaxial Young's modulus along the c-axis was independently determined from simulated tensile tests. Young's moduli for 3C- and 6H-SiC are plotted as a function of temperature in Figure 5. Our analysis reveals a notablestriking difference in high-temperature stability of their values. The cubic 3C polytype exhibits a markedly superior stiffness retention, with its Young's modulus degrading at a rate of approximately 25 MPa/K — nearly half the rate observed for the 6H polytype, which softens at approximately 49 MPa/K. As discussed in Section 3.3, the VRH-averaged polycrystalline estimate yields a common softening rate of ~33 MPa/K for both polytypes, masking this direction-dependent anisotropy — a distinction that underscores the complementary value of uniaxial and polycrystalline characterization approaches.

This finding points to a critical trade-off between thermodynamic stability and mechanical performance in SiC polytypes. For high temperature applications hexagonal polytypes are generally preferred due to their superior thermodynamic stability. It is well-established experimentally that the cubic 3C form can undergo an irreversible transformation to the 6H structure when subjected to thermal annealing[32]. However, our results demonstrate a compelling counterpoint: within its stable operational temperature range, 3C-SiC is mechanically more robust, exhibiting a significantly better retention of stiffness than its hexagonal counterpart. This specific conclusion is in agreement with Xu et al.[31] that has also predicted a more pronounced thermal softening in the hexagonal polytypes compared to the cubic form.

4. Conclusion

In this work, we have performed a systematic and comparative investigation of the thermo-mechanical properties of 3C- and 6H-SiC using large-scale molecular dynamics simulations with a high-fidelity Machine Learning Interatomic Potential trained on custom DFT data. The potential was rigorously validated against 0 K DFT and experimental data before being deployed for finite-temperature calculations.

We have successfully calculated the coefficient of thermal expansion, the full set of temperature-dependent elastic constants, and the effective polycrystalline Young's and bulk moduli for both polytypes from 0 K to 2000 K. Our results provide a quantitative picture of thermal softening, showing a near-linear decrease in stiffness with increasing temperature. A comparative analysis demonstrates a crucial finding: the Young's modulus of single-crystal 6H-SiC decreases with increasing temperature almost twice as fast as that of the 3C polymorph, highlighting a significant trade-off between room-temperature rigidity and high-temperature mechanical stability.

The presented work proposes a validated computational framework and a self-consistent, high-fidelity dataset of thermo-mechanical properties for two of the most important SiC polytypes. This data is critical for improving the accuracy of multi-scale material models and will aid in the design, analysis, and lifetime prediction of SiC components for challenging high-temperature applications. Furthermore, the large scale of the systems studied here provides a solid basis for future studies of the influence of point defects, such as widespread impurities or vacancies, on the thermo-mechanical behavior of SiC.

References

1. Y. Katoh, L.L. Snead, C.H. Henager, et al., Current status and recent research achievements in SiC/SiC composites, J. Nucl. Mater. 455 (2014) 387 – 397. https://doi.org/10.1016/j.jnucmat.2014.06.003.
2. D.E. Glass, Ceramic Matrix Composite (CMC) Thermal Protection Systems (TPS) and Hot Structures for Hypersonic Vehicles, in: 15th AIAA International Space Planes and Hypersonic Systems and Technologies Conference, 2008. https://doi.org/10.2514/6.2008-2682.
3. B.J. Baliga, Silicon Carbide Power Devices, in: M. Rudan, R. Brunetti, S. Reggiani (Eds.), Springer Handbook of Semiconductor Devices, Springer, 2022. https://doi.org/10.1007/978-3-030-79827-7_14.
4. G.L. Harris, Properties of Silicon Carbide, INSPEC, the institution of electrical engineers, London, 1995.
5. G.E. Mase, G.T. Mase, Continuum Mechanics for Engineers, second ed., CRC Press, Boca Raton, 1999.
6. C. Kittel, Introduction to Solid State Physics, eighth ed., Wiley, Hoboken, 2004.
7. J.P. Hirth, J. Lothe, Theory of Dislocations, second ed., Wiley, New York, 1982.
8. P. Vashishta, R.K. Kalia, A. Nakano, J.P. Rino, Interaction potential for silicon carbide: A molecular dynamics study of elastic constants and fracture, amorphization, and nanoindentation,

J. Appl. Phys. 101 (2007) 103515. https://doi.org/10.1063/1.2724570.
9. J. Behler, Perspective: Machine learning potentials for atomistic simulations, J. Chem. Phys. 145 (2016) 170901. https://doi.org/10.1063/1.4966192.
10. S. Batzner, A. Musaelian, L. Sun, et al., E(3)-equivariant graph neural networks for data-efficient and accurate interatomic potentials, Nat. Commun. 13 (2022) 2453. https://doi.org/10.1038/s41467-022-29939-5.
11. J.P. Perdew, K. Burke, M. Ernzerhof, Generalized Gradient Approximation Made Simple, Phys. Rev. Lett. 77 (1996) 3865. https://doi.org/10.1103/PhysRevLett.77.3865.
12. G. Kresse, D. Joubert, From ultrasoft pseudopotentials to the projector augmented-wave method, Phys. Rev. B. 59 (1999) 1758 – 1775. https://doi.org/10.1103/PhysRevB.59.1758.
13. A.H. Larsen, J.J. Mortensen, J. Blomqvist, et al., The atomic simulation environment—a Python library for working with atoms, J. Phys. Condens. Matter. 29 (2017) 273002. https://doi.org/10.1088/1361-648X/aa680e.
14. D. Frenkel, B. Smit, Understanding Molecular Simulation: From Algorithms to Applications, second ed., Academic Press, Cambridge, 2002.
15. R. Hill, The elastic behaviour of a crystalline aggregate, Proc. Phys. Soc. A 65 (1952) 349. https://doi.org/10.1088/0370-1298/65/5/307.
16. Z.J. Wu, E.J. Zhao, H.P. Xiang, X.F. Hao, X.J. Liu, J. Meng, Crystal structures and elastic properties of superhard IrN_2 and IrN_3 from first principles, Phys. Rev. B. 76 (2007) 054115. https://doi.org/10.1103/PhysRevB.76.054115.
17. M. Prikhodko, M.S. Miao, W.R.L. Lambrecht, Pressure dependence of sound velocities in 3C−SiC and their relation to the high-pressure phase transition, Phys. Rev. B. 66 (2002) 125201. https://doi.org/10.1103/physrevb.66.125201.
18. W.R.L. Lambrecht, B. Segal, A. Methfessel, M. Schilfgaard, Calculated elastic constants and deformation potentials of cubic SiC, Phys. Rev. B. 44 (1991) 3685 – 3694. https://doi.org/10.1103/PhysRevB.44.3685.
19. W.H. Lee, X.H. Yao, First principle investigation of phase transition and thermodynamic properties of SiC, Comput. Mater. Sci. 106 (2015) 76 – 82. https://doi.org/10.1016/j.commatsci.2015.04.044.
20. P. Djemia, Y. Roussigné, G.F. Dirras, K.M. Jackson, Elastic properties of nanocrystalline silicon carbide films, J. Appl. Phys. 95 (2004) 2324 – 2330. https://doi.org/10.1063/1.1642281.
21. S.Q. Wang, H.Q. Ye, Ab initio elastic constants for the lonsdaleite phases of C, Si and Ge, J. Phys. Condens. Matter. 15 (2003) 5307 – 5314. https://doi.org/10.1088/0953-8984/15/30/312.
22. K. Kamitani, M. Grimsditch, J.C. Nipko, C.K. Loong, M. Okada, I. Kimura, The elastic constants of silicon carbide: A Brillouin-scattering study of 4H and 6H SiC single crystals, J. Appl. Phys. 82 (1997) 3152 – 3154. https://doi.org/10.1063/1.366100.
23. G. Arlt, G.R. Schodder, Some elastic constants of silicon carbide, J. Acoust. Soc. Am. 37 (1965) 384 – 386. https://doi.org/10.1121/1.1909336.
24. N.M. Sultan, T.M.B. Albarody, H.K.M. Al-Jothery, M.A. Abdullah, H.G. Mohammed, K.O. Obodo, Thermal expansion of 3C-SiC obtained from in-situ X-ray diffraction at high temperature and first-principal calculations, Materials. 15 (2022) 6229. https://doi.org/10.3390/ma15186229.
25. Z. Li, R.C. Bradt, Thermal Expansion of the Hexagonal (6H) Polytype of Silicon Carbide, J. Am. Ceram. Soc. 69 (1986) 863 – 866. https://doi.org/10.1111/j.1151-2916.1986.tb07385.x.
26. H. Rabiee, Temperature and pressure dependence on mechanical properties and defect formation structure in 3C-SiC: A molecular dynamics study, Results Eng. 26 (2025) 104734. https://doi.org/10.1016/j.rineng.2025.104734.
27. R.R. Reeber, K. Wang, High Temperature Elastic Constant Prediction of Some Group-III Nitrides, MRS Internet J. Nitride Semicond. Res. 6 (2001). https://doi.org/10.1557/S1092578300000156.
28. J.B. Wachtman, W.E. Tefft, D.G. Lam, C.S. Apstein, Exponential Temperature Dependence of Young's Modulus for Several Oxides, Phys. Rev. 122 (1961) 1754 – 1759. https://doi.org/10.1103/PhysRev.122.1754.
29. J.I. Im, B.W. Park, H.Y. Shin, J.H. Kim, Temperature Dependence on Elastic Constant of SiC Ceramics, J. Korean Ceram. Soc. 47 (2010) 491. https://doi.org/10.4191/kcers.2010.47.6.491.
30. Z. Li, R.C. Bradt, The single-crystal elastic constants of cubic (3C) SiC to 1000°C, J. Mater. Sci. 22 (1987) 2557 – 2559. https://doi.org/10.1007/BF01082145.
31. W.W. Xu, F. Xia, L. Chen, M. Wu, T. Gang, Y. Huang, High-temperature mechanical and thermodynamic properties of silicon carbide polytypes, J. Alloys Compd. 768 (2018) 722 – 732. https://doi.org/10.1016/j.jallcom.2018.07.299.
32. A. Boulle, J. Aubé, I.G. Galben-Sandulache, D. Chaussende, The 3C-6H polytypic transition in SiC as revealed by diffuse x-ray scattering, Appl. Phys. Lett. 94 (2009) 201904. https://doi.org/10.1063/1.3141509.